ESOMAT 2009, 04007 (2009)
DOI:10.1051/esomat/200904007

In-situ TEM straining of tetragonal martensite of Ni-Mn-Ga alloy

Yanling Ge[a], Niva Zárubová[1], Zdeněk Dlabáček[1], Ilkka Aaltio[a], Outi Söderberg[a], Simo-Pekka Hannula[a]

Department of Materials Science and Engineering, Helsinki University of Technology, P.O. Box 6200, FI-02015 TKK, Finlad
[1] Institute of Physics, ASCR v.v.i., Na Slovance 2, 182 21 Prague 8, Czech Republic

Abstract. The *in-situ* straining of tetragonal martensite of Ni-Mn-Ga alloy was studied in a transmission electron microscope (TEM) JEM 1200EX equipped with a double tilt straining stage. The sample was analyzed before and after the straining experiments using the conventional as well as high resolution TEM (Tecnai F20 G2 200kV FEG). Before straining, the martensitic structure of the samples consisted of thermally induced self-accommodated multi-variants. During the *in-situ* straining, detwinning processes were recorded. The volume fraction of the twin variants preferably oriented to the applied tensile force increased at the expense of the less favorably oriented ones. The movement of the twin boundaries was followed in detail. The analysis performed after straining suggested that the detwinning processes occurred by movement of twinning dislocations. The interface between two twinned bands acted as a nucleation source for emitting the twinning dislocations.

1. Introduction

Ni-Mn-Ga alloy is a ferromagnetic shape memory alloy (FSMA) which transforms from the cubic high temperature phase to thermoelastic martensite and undergoes a magnetic transition during cooling [1-2]. This alloy has been extensively studied because of a variety of remarkable properties, such as magnetic-field-induced-strain (MFIS) [3], superelasticity [4], thermally induced shape memory effect [6], magnetoresistance[6], and magnetocaloric behavior [7]. In alloys of certain compositions, the martensitic twin structure is coupled with magnetic domains in such a way that the magnetic field can reorient martensitic twin variants, which results in a giant straining [8]. In this context the mobility of twin boundary motion is a critical factor. It is also of great importance when considering superelasticity and thermally induced shape memory effect in this material. These phenomena may exist in the non-modulated tetragonal Ni-Mn-Ga martensite, though the magnetically induced reorientation of the martensite twins is not very likely to occur [9]. In the present work, *in-situ* TEM observations were carried out to understand the twinning and detwinning processes occurring in the tetragonal Ni-Mn-Ga martensite. The studied alloy with a non-modulated structure exhibits about 19% strain under stress by reorientation of martensitic twin variants [10]. In modulated martensites, the same reorientation yields only 6 to 10 % depending on the crystallographic structure of the material, but the reorientation can be induced also by the magnetic field, in addition to the stress, in those alloys. The mechanism of the twin boundary motion is the same both for magnetic stress and mechanical stress in the modulated martensites [11]. It is thus reasonable to assume that the stress induced twin boundary motion in the non-modulated martensite could give insight also into the mechanism of magnetically induced twin boundary movement in modulated martensites.

2. Experimental

The crystal structure and lattice parameters of the studied $Ni_{52.4}Mn_{27.3}Ga_{20.3}$ alloy were determined by the X'pert MRD with $Co_{K\alpha}$ radiation. The samples for straining in TEM were cut from a plate with [001] normal in the austenite state and wet ground to dimensions of 1.67mm x 5.5mm x 0.5mm. In the final stage, the central area of the sample was thinned in a Fischione double jet polisher (30% solution of HNO_3 in methanol, -40^oC) to get a hole. The sample was strained in tension at room temperature in a JEM 1200EX microscope equipped with a double tilt straining stage (x-tilt ±30°, y-tilt ±10°, load max. 25 N) constructed in the Institute of Physics of the ASCR [12]. The specimen was observed during straining under two-beam bright field conditions and the

[a] e-mail: yanling.ge@tkk.fi

Article available at http://www.esomat.org or http://dx.doi.org/10.1051/esomat/200904007

transformation processes were video-recorded by a Mega View III camera. The straining was finished after a crack had appeared in the sample. The highest load applied in the experiments was 3.8 N. A detailed structural study of the tested sample was carried out under stress in the JEM 1200EX TEM. Then the long tensile foil was cut to a 3 mm disc to fit into a normal double tilt holder and examined in the high-resolution transmission electron microscope Tecnai F20 G2 equipped with GIF tridiem.

3. Results and discussion

The transition temperatures of the studied $Ni_{52.4}Mn_{27.3}Ga_{20.3}$ alloy were M_s = 397.9 K, M_f = 391.3 K, A_s = 402.5 K, A_f = 407.9 K, and T_c = 380.2 K. At room temperature the specimen had a tetragonal martensitic crystal structure with the lattice parameters of a = 5.49 Å and c = 6.61 Å while the high temperature cubic austenite had a = 5.84 Å at 419 K. For a cubic to tetragonal transformation there are three possible correspondence martensite variants with their lattice vectors parallel to the edges of the cubic unit cell. The martensite lattice vectors are in correspondence with the austenite lattice as listed in Table 1.

Table 1. Lattice vector correspondence between austenite and martensite.

Martensite variant	$[100]_M$	$[010]_M$	$[001]_M$
M1	$[010]_A$	$[001]_A$	$[100]_A$
M2	$[001]_A$	$[100]_A$	$[010]_A$
M3	$[100]_A$	$[010]_A$	$[001]_A$

The twin planes $\{101\}_M$ of martensite are derived from the six $\{101\}_A$ planes in austenite and therefore there are six pairs of martensite variants. The situation is illustrated in Fig. 1b. Due to the rotation during the martensitic phase transformation each martensite variant can occur in two orientations, M and M' which combine on different twin planes. The six possible martensite variant combinations are indicated, together with the traces of the corresponding twin planes on $(001)_A$ plane, in Fig. 1a. As the martensite structure of the studied sample was formed in the thermal phase transformation, all six combinations of the three martensite variants were found in it. The selected area electron diffraction (SAED) patterns of the three martensite variants are shown in Fig. 1c. The length dimension of the sample was parallel to the X-direction of the stage (direction of the external load). As it can be seen from Fig. 1a, the angle between the long $[001]_M$ lattice vector and the external stress axis was the smallest for variant M2 which was thus the most favorably oriented variant under stress. Variant M3 was the least favorable one.

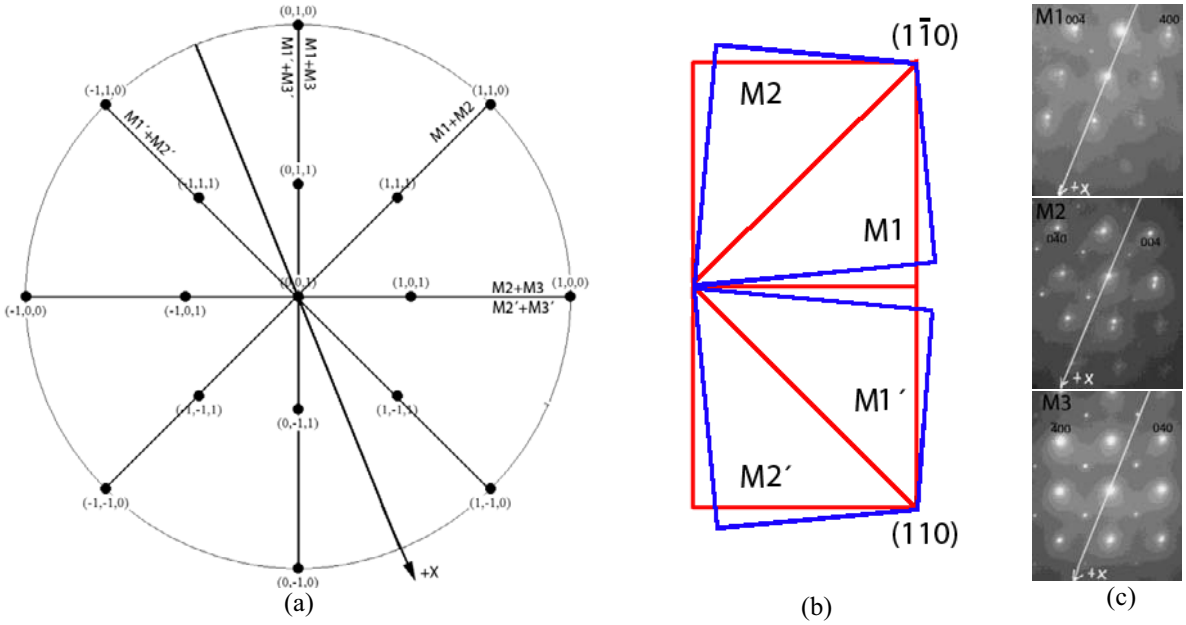

Fig. 1. (a) Stereo projection of the sample (drawn in the austenite lattice for simplicity): The orientations of the six twin planes for six possible variant combinations are given. The traces of the twin planes on the (001) foil surface are marked. The +X direction is the X axis of the sample holder and direction of the external load. (b) A schematic of two possible combinations of the same martensite variants. M1, M1´ have identical correspondence to the austenite but combine with M2, M2' on different habit planes. (c) The selected area electron diffraction (SAED) patterns of three martensite variants.

The strained area shown in Fig. 2 was selected near the hole, in the region of the maximum stress in the sample [13]. There are three bands with the internal twins marked as A, B and C in Fig. 2a. The electron diffraction pattern made before straining indicated that bands A and B consisted of variants M2 + M3, band C of M1 + M3. The applied tensile force was increased gradually to 3.8 N and then it was kept at that value. The video was recorded from the beginning of loading until a crack appeared in the sample. When the straining started, some of the internal twins moved at a high speed in band B. As this happened very fast, no single dislocation movement could be distinguished. After 10.40 minutes, dislocations started shooting at the interface between bands B and C into both bands B and C. The twinning dislocation front is seen as a bow contrast with stacking fault fringes behind them (Figs. 2b, d). The detwinning process is carried out plate by plate, and the total disappearance of one plate needs numerous twinning dislocations passing through. In Fig. 2b some of the twin plates have already disappeared, some are disappearing, and some are just starting to disappear. After 26 minutes (Fig. 2c) band C has become one martensite variant except for a few twin plates locked by some lattice dislocation. Also these twin plates were released at the end of the process (Fig. 2d). It should be noted that new lattice dislocations were formed during the detwinning process and left behind, such as the dislocation lines lying next to the BC band interface and parallel to it in band B, and piles of dislocations in band C (Fig. 2d). Fig. 2d was taken after the load had been decreased to 2 N. It shows that band C is now formed nearly totally of variant M1 (confirmed by SAED) while a few thin plates still remain in band B. When the sample was reloaded to 3.3 N, the remaining plates got released and only two plates are left (Fig. 2e) in band B. After 5 minutes straining with 3.3 N, all plates disappeared in band B (Fig. 2f). The band B consists now of variant M2, as indicated by SAED. The new plates parallel to the band interface that started to form in band C after reloading to 3.3 N (Fig. 2e), were identified by SAED as variant M2. Referring to Fig. 1, the interface between bands B and C fits nearly perfectly to the twin plane of M1'+ M2'.

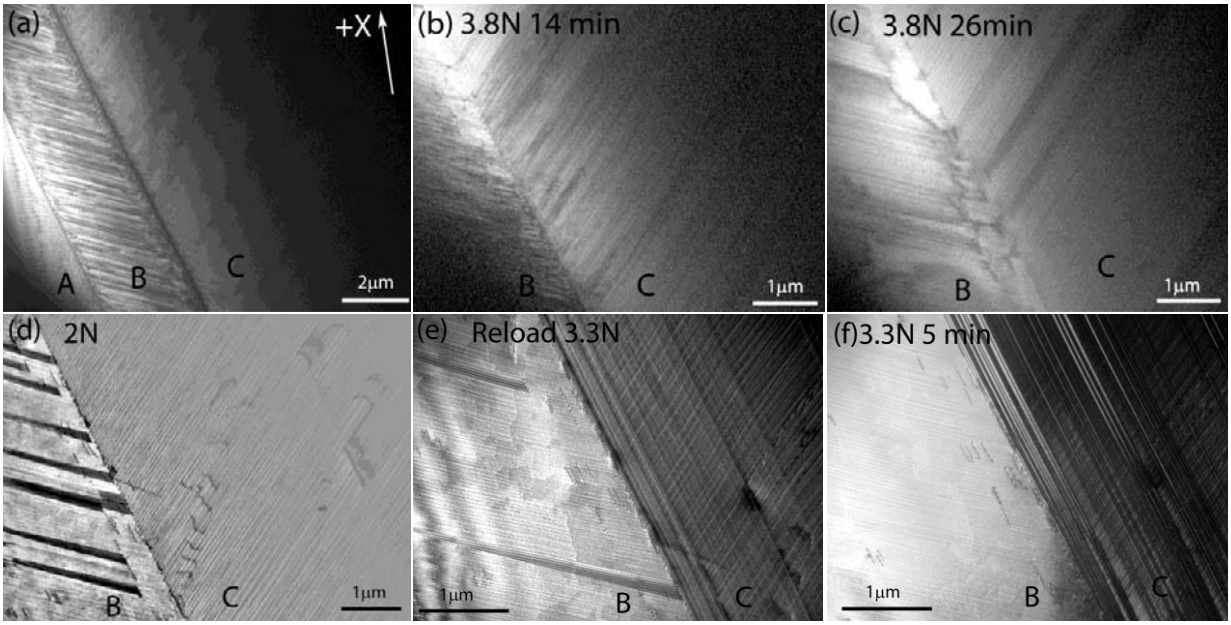

Fig. 2. (a) – (c) are frames from the video-record of the straining. (a) The start frame, (b) after 14 minutes loading at 3.8 N, and (c) after 26 minutes loading at 3.8 N. (d) The load is decreased to 2 N, and (e) reloaded to 3.3 N, and (f) the load of 3.3 N has been applied for 5 minutes.

It is apparent from the video-records that twinning dislocations were emitted from the band interface during detwinning process, i.e., the band interface is a source of twinning dislocations. The twinning dislocations were curved when they moved under stress. In the high resolution TEM study carried out after straining, some twinning dislocations were still found. Since there was no stress influencing the sample, the dislocation curvature was clearly smaller than that under stress. In Fig. 3 the bright field (BF) images of the remaining twinning dislocations were taken under two beam conditions with four reflections, $0\bar{2}2$, $0\bar{4}0$, 022 and 004, of the M2 structure. These images show clearly stacking fault fringes, an overlap of the stacking fault contrast, and changes of the stacking fault fringes due to twinning dislocations. The stacking fault fringe contrast behind twinning dislocations suggests that they are partial dislocations. Only reflection $0\bar{4}0$ gives no contrast for twinning dislocation (Fig. 3b). Also the lattice dislocation lying in the lower-left corner shows a weak contrast. Since the twinning dislocation must glide on the twin plane, both the dislocation line and the Burgers vector are in the twin plane. In Fig. 3, the twin plane $(101)_{M2}$ is inclined to the sample surface since the zone axis for the symmetry

diffraction is $[100]_{M2}$. The reflection $0\bar{4}0$ is perpendicular to the twin plane $(101)_{M2}$, and thus it must be perpendicular to the twinning dislocations lines and their Burgers vectors. Since the lattice dislocation lines are formed during detwinning process, it is very likely that they also lie in the twin plane, and the weak contrast may suggest that it fulfills the invisibility criterion for an anisotropic material. It would be more helpful to use reflection 101 for the imaging but unfortunately it was not possible due to the tilt limitation of the equipment. Therefore, further investigation the Burgers vectors of the twinning dislocations with some special technique will be carried out in future studies.

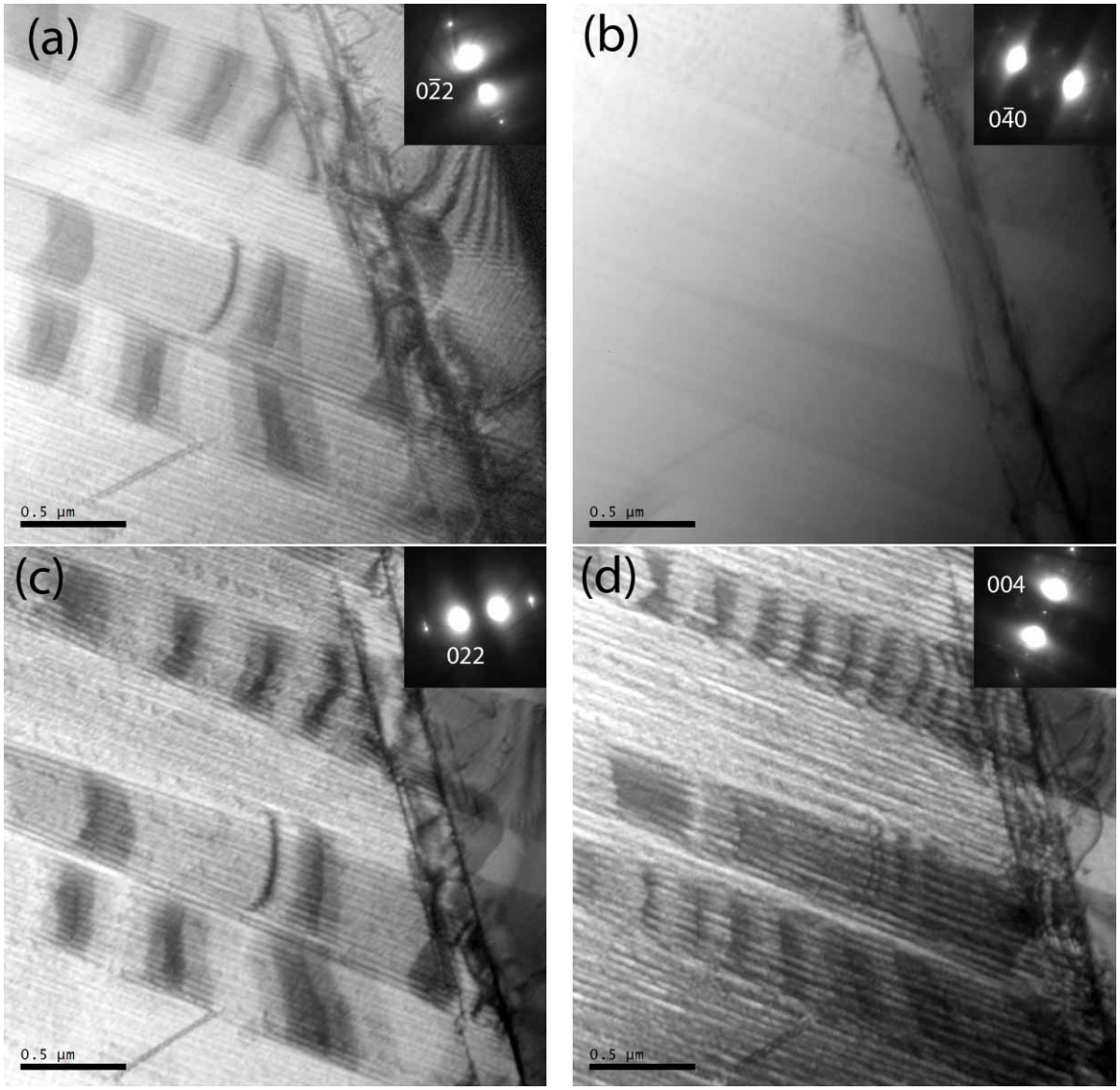

Fig. 3. BF images of the twinning dislocations with different reflections under two beam conditions in the high resolution TEM study. The insets are corresponding reflections (indexed in M2) used in the image.

4. Conclusions

The *in-situ* TEM tensile study and high resolution TEM investigation with the same sample were performed on a non-modulated Ni-Mn-Ga alloy. It was found that the detwinning process of the martensite is implemented through the plate by plate transformation of one martensite variant into the other. This process occurs via movement of twinning dislocations. Existing interface between two twinned bands acts as a source of the twinning dislocations. Stacking faults fringes are associated with the twinning dislocations showing that they are partial dislocations.

Acknowledgement

The authors highly acknowledge the financial support of the Academy of Finland and of the Grant Agency of ASCR (contract No. A200100627).

References

[1] P.J. Webster, Philos. Mag. B **49**, 295 (1984)
[2] V. V. Martynov and V. V. Kokorin, J Phys. III **2**, 739 (1992
[3] K. Ullakko, J. K. Huang, C. Kantner, R. C. O'Handley and V. V. Kokorin, Appl. Phys. Lett. **69**, 1966 (1996)
[4] V.A. Chernenko, V. L'vov, J. Pons and E. Cesari, J Appl. Phys. **93**, 2394 (2003)
[5] H.B. Xu, Y.Q. Ma and C.B. Jiang, , Appl Phys Lett **82**, 3206 (2003)
[6] C. Biswas, R. Rawat and S. Barman, Appl. Phys. Lett. **86**, 202508 (2005)
[7] V. Shavrov, T. Takagi, J. Magn. Magn. Mater. **272–276**, 2040 (2004)
[8] Y. Ge, O. Heczko, O. Söderberg and V.K. Lindroos, J Appl Phys **96**, 2159 (2004)
[9] A. Sozinov, A.A. Likhachev, N. Lanska, O Söderberg, K. Koho, K. Ullakko, V.K. Lindroos, J. Phys. IV Fr. Proc. **115**, 121 (2004)
[10] O. Söderberg, L. Straka, V. Novák, O. Heczko, S.-P. Hannula and V.K. Lindroos, Mater. Sci. Eng. A **386**, 27 (2004)
[11] A. Sozinov, A.A. Likhachev, N. Lanska, K. Ullakko, Appl. Phys. Lett. **80** 1746 (2002)
[12] Z. Dlabáček, A. Gemperle, J. Gemperlová, "Improved design of a double tilt side entry straining stage for TEM", 13th Electron Microscopy Congress, Antwerp 2004, edited by D. Schryvers and J.-P. Timmermans, p. 417
[13] A. Coujou, Ph. Lours, N.A. Roy, D. Caillard, N. Clement, Acta Metall. **38**, 825 (1990)